A 'GAS OF CIRCLES' PHASE FIELD MODEL AND ITS APPLICATION TO TREE CROWN EXTRACTION

Péter Horváth[1], *Ian H. Jermyn*[2]

[1] University of Szeged, Institute of Informatics, P.O. Box 652,
H-6701 Szeged, Hungary, Fax:+36 62 546 397,
[2] Ariana (INRIA/I3S), INRIA,
B.P. 93, 06902 Sophia Antipolis, France, Fax:+33 4 92 38 76 43

ABSTRACT

The problem of extracting the region in the image domain corresponding to an a priori *unknown number of circular objects occurs in several domains. We propose a new model of a 'gas of circles', the ensemble of regions in the image domain composed of circles of a given radius. The model uses the phase field reformulation of higher-order active contours (HOACs). Phase fields possess several advantages over contour and level set approaches to region modelling, in particular for HOAC models. The reformulation allows us to benefit from these advantages without losing the strengths of the HOAC framework. Combined with a suitable likelihood energy, and applied to the tree crown extraction problem, the new model shows markedly improved performance, both in quality of results and in computation time, which is two orders of magnitude less than the HOAC level set implementation.*

1. INTRODUCTION

Forestry services (for example, the National Forest Inventory in France) are interested in various statistics associated with forests and plantations, such as the density of trees, the mean crown area and diameter, and so forth. These statistics are very useful for the management of resources and the conservation of forestry areas. Acquiring this data is, however, expensive, requiring field surveys or semi-automatic extraction of the necessary information from remote sensing images. If the region in the image domain corresponding to tree crowns could be extracted automatically from remote sensing images, many of the statistics could be computed automatically, and a great deal of time and money could be saved. As a consequence, the tree crown extraction problem is of some importance to forestry institutions.

Horváth et al. [4] addressed this problem using the higher-order active contour (HOAC) framework [9, 11]. HOACs are a new generation of active contour models [5] allowing the incorporation of non-trivial prior knowledge about region geometry, and the relation between region geometry and the data, via nonlocal interactions between tuples of region boundary points. They differ from most other methods for incorporating prior geometric knowledge into active contours, for example [1, 2, 7], in not being based upon perturbations of a reference region or regions. In consequence, they can detect multiple instances of an entity at no extra cost, a critical requirement for the current application. [9, 11] applied the HOAC framework to the road network extraction problem using a prior model favouring (*i.e.* assigning low energy to) regions composed of thin arms meeting at junctions.

In order to solve the tree crown extraction problem, Horváth et al. [4] extended the range of the HOAC framework by introducing a model of a 'gas of circles'. The HOAC 'gas of circles' model favours regions in the image domain consisting of a set of circles with a given radius (see the rightmost column of figure 1 for some examples). In conjunction with a suitable likelihood energy, the model works well for tree crown extraction, but suffers from some drawbacks. In particular, the computation time is long. Each iteration of the gradient descent algorithm used to minimize the model energy takes time proportional to the square of the length of the region boundary, and in addition involves complex computations. When many tree crowns are present, the region boundary is long, hence so is computation time.

Rochery et al. [10] introduced an alternative formulation of HOAC models, based on the 'phase field' framework much used in physics to model regions and interfaces. The standard phase field model is, to a good approximation, equivalent to a classical active contour (CAC) model with energy given by boundary length. Rochery et al. [10] showed how to extend the basic phase field energy with extra, nonlocal terms that produce phase field models equivalent to higher-order active contours. The reason for being interested in an equivalent formulation of the same family of models is that the new formulation has several important advantages:

- Phase field models provide a neutral initialization for gradient descent—no initial region is needed—meaning that bias caused by the initialization is reduced.
- The implementation of the phase field version of CACs, and in particular of HOACs, is much simpler than the equivalent contour or level set implementation. Gradient descent consists of a single partial differential equation derived directly from the model energy with no need for reinitialization or regularization. HOAC terms consist of convolutions and can be evaluated in Fourier space.
- There is more topological freedom during the gradient descent evolution than with other methods, which is important when the topology is unknown *a priori* as is the case in the tree crown extraction problem. In addition, more topological freedom means less chance of becoming stuck in local minima.
- The computation time does not depend on the complexity of the region, and for most problems we have examined, is an order of magnitude faster for HOACs than the level

THIS WORK WAS PARTIALLY SUPPORTED BY EU PROJECT MUSCLE (FP6-507752), EGIDE PAI BALATON, OTKA T-046805, AND A HAS JANOS BOLYAI RESEARCH FELLOWSHIP. WE THANK THE FRENCH NATIONAL FOREST INVENTORY (IFN) FOR THE DATA.

set implementation.

Rochery et al. [10] applied the phase field version of their HOAC network model to the road network extraction problem. The purpose of the present paper is to address the tree crown extraction problem by constructing a phase field model of a 'gas of circles'.

In section 2, we briefly recall the HOAC 'gas of circles' model, while in section 3, we introduce the phase field 'gas of circles' model. One of the key elements of the HOAC 'gas of circles' model is the stability calculation that furnishes model parameter values that guarantee that the energy favours circles of a given radius that are stable to all small perturbations. In section 4, we compute, as a function of the HOAC energy parameters, the phase field energy parameters that produce an equivalent model. This means that we can adjust the phase field parameters to ensure stable circles of a given radius also. We demonstrate the correctness of these calculations, and the nature of the resulting model, with experiments.

In section 5, we describe a suitable likelihood energy for the tree crown extraction problem, and in section 6, we present results on colour infrared aerial images obtained using this likelihood in conjunction with the phase field 'gas of circles' model. We compare our results with the results obtained using a CAC model and the HOAC 'gas of circles' model. We find that the results are more accurate, while computation time is greatly reduced. We conclude in section 7.

2. THE 'GAS OF CIRCLES' MODEL

HOAC energies generalize CAC energies by including multiple integrals over the region boundary. The simplest such generalizations are quadratic energies, which contains double integrals. There are several forms that such multiple integrals can take, depending on whether or not they take into account boundary direction at the interacting points. The Euclidean invariant version of one of these forms, introduced by Rochery et al. [9], is

$$E_{C,\mathrm{G}}(R) = E_{C,0}(R) + E_Q(R) = \lambda_C L(\partial R) + \alpha_C A(R) - \frac{\beta_C}{2} \iint dp\, dp'\, \dot{\gamma}(p) \cdot \dot{\gamma}(p')\, \Psi(\sigma(p,p')/d) \ , \quad (1)$$

where R is a region in the image domain and ∂R is its boundary; γ is a member of the equivalence class of maps representing the region boundary and p is a coordinate on its domain; dot indicates derivative with respect to p; L is the boundary length functional; A is the region area functional; $\sigma(p,p') = |\gamma(p) - \gamma(p')|$; and Ψ is an interaction function that determines the geometric content of the model.

With an appropriate choice of Ψ, the quadratic term creates a repulsion between nearby antiparallel tangent vectors. This has two effects. First, for particular ranges of α_C and β_C (λ_C and d can be set equal to 1 merely by changing our length and energy units), circular structures, with a radius r_0 dependent on the parameter values, are stable to perturbations of their boundary. Second, such circles repel one another if they approach closer than $2d$. Regions consisting of collections of circles of radius r_0 separated by distances greater than $2d$ are thus local energy minima. Horváth et al. [4] call this the 'gas of circles' model. Via a stability analysis, they found the ranges of parameter values rendering circles of a given radius stable as functions of the desired radius.

To illustrate the information contained in $E_{C,\mathrm{G}}$, the first row of figure 1 shows the result of gradient descent using $E_{C,\mathrm{G}}$ starting from the region on the left. Note the production of stable circles of the prescribed radius.

3. PHASE FIELD MODEL

Rochery et al. [10] introduced a phase field version of the above HOAC model. A phase field ϕ is a real-valued function on the image domain Ω. Given a threshold z, there is a map ζ from the space of functions Φ to the space of regions in the image domain given by $\zeta_z(\phi) = \{x \in \Omega : \phi(x) > z\}$. Thus phase fields are a level set representation, but the functions are not constrained: Φ is a linear space. The simplest phase field energy is

$$E_0(\phi) = \int_\Omega dx \left\{ \frac{D}{2} \partial\phi \cdot \partial\phi + \lambda(\frac{1}{4}\phi^4 - \frac{1}{2}\phi^2) + \alpha(\phi - \frac{1}{3}\phi^3) \right\} .$$

If D were 0, the second line would mean that $\phi_R \triangleq \arg\min_{\phi:\, \zeta_z(\phi)=R} E_0(\phi)$, *i.e.* the minimizing phase field for a given fixed region, would take the value 1 inside R and -1 outside. The effect of $D \neq 0$ is to smooth this scaled, shifted characteristic function so that it has an interface of finite width centred around ∂R. The phase field model is approximately[1] equivalent to a CAC in the sense that

$$E_0(\phi_R) \approx \lambda_C L(\partial R) + \alpha_C A(R) = E_{C,0}(R) \ , \quad (2)$$

where α_C and λ_C are given approximately by $\alpha_C = 4\alpha/3$ and $\lambda_C^2 = 16D\lambda K/15$ where $K = 1 + 5(\alpha/\lambda)^2$. The width of the interface is given by $w = 4D/\lambda_C$. Equation (2) means that gradient descent with the phase field model E_0 will be equivalent to gradient descent with the contour energy $E_{C,0}$, equivalence being defined by ζ.

To create a model equivalent to $E_{C,\mathrm{G}}$, Rochery et al. [10] added the following nonlocal phase field term to E_0:

$$E_{NL}(\phi) = -\frac{\beta}{2} \int_{\Omega^2} dx\, dx'\, \partial\phi(x) \cdot \partial\phi(x')\, G(x - x') \ , \quad (3)$$

where $G(x-x') = \Psi(|x-x'|/d)$. They show that the relation between the parameters for model equivalence is $\beta_C = 4\beta$.

With the parameters thus translated, the phase field model $E_\mathrm{G} = E_0 + E_{NL}$ is equivalent (as usual, to a good approximation) to the HOAC model $E_{C,\mathrm{G}} = E_{C,0} + E_Q$, and can be used in its place, thus allowing the incorporation of non-trivial prior knowledge about region geometry while still profiting from all the advantages of the phase field framework.

4. 'GAS OF CIRCLES' PHASE FIELD MODEL

Horváth et al. [4] showed via a stability analysis of the energy $E_{C,\mathrm{G}}$ how the parameters of the HOAC model should be chosen so that it favours regions consisting of sets of circles with a prescribed radius. In this section, we show how the same can be done for the phase field formulation.

First we need to invert the expressions for the phase field parameters in terms of the HOAC parameters. Clearly $\alpha =$

[1] For a detailed discussion of why the approximation error does not matter, see [10].

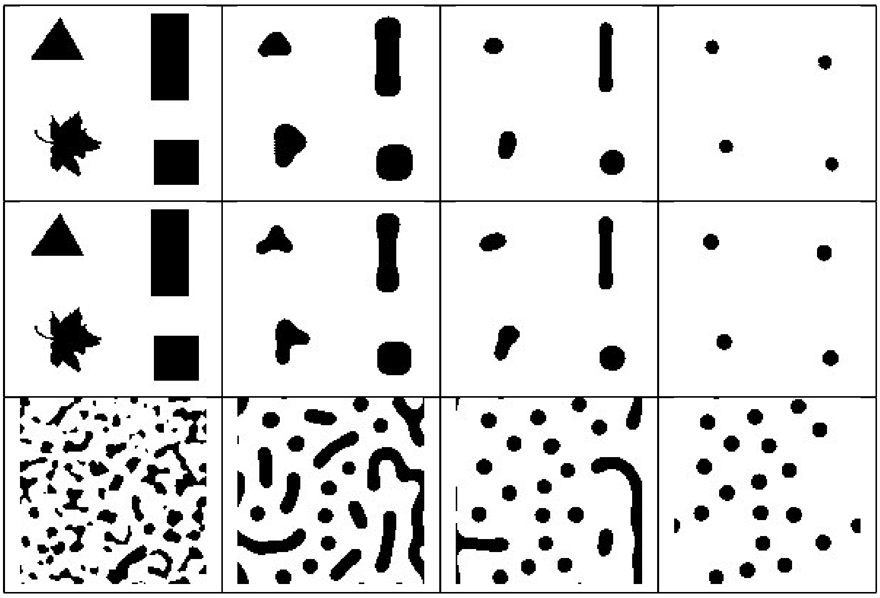

Figure 1: First row: gradient descent using $E_{C,\mathrm{G}}$ ($\lambda_C = 10$, $\alpha_C = 1$, $\beta_C = 2.3137$, $r_0 = 5$). Second and third rows: gradient descent using E_{G}, with parameters equivalent to those used in the first row ($\lambda = 9.064$, $\alpha = 0.75$, $\beta = 0.5784$, $D = 10$, $r_0 = 5$). The initialization used in the second row was equivalent to that used in the first row, while in the third row the neutral initialization was used with a small amount of added Gaussian noise. Time runs from left to right.

$3\alpha_C/4$ and $\beta = \beta_C/4$. It is slightly more difficult to compute λ. It turns out to be simplest to use the interface width w as a parameter instead of D (recall that $w = 4D/\lambda_C$). There are in principle two solutions, given by

$$\tilde{\lambda}_\pm = \frac{\lambda_\pm}{\lambda_C} = \frac{15}{8w}\left[1 \pm \sqrt{1 - 4\tilde{\alpha}_C{}^2 w^2/5}\right], \qquad (4)$$

where $\tilde{}$ denotes division by λ_C. In practice, we choose λ_+, because this is the branch of the solution consistent with $\alpha_C = 0$. Note that this equation imposes a constraint on α_C for there to be a solution: $\tilde{\alpha}_C \leq \sqrt{5}/(2w)$. Finally, $D = \lambda_C w/4$. Note that for fixed $\tilde{\alpha}_C$ and $\tilde{\beta}_C$, the effect of λ_C is simply to scale all the phase field parameters.

We can take the following steps to create a phase field 'gas of circles' model for a prescribed radius r_0. (We assume that units have been chosen so that $d = 1$. If other units are chosen, *e.g.* pixel units, the parameters must be rescaled.)

- Choose w. It cannot be too small, or a subpixel discretization will be needed for gradient descent, and it cannot be too large or the phase field model will not be a good approximation to the HOAC model [10]. We have found that $w = 3$ or $w = 4$ work well.
- Equation (4) now determines an upper bound on $\tilde{\alpha}_C$. Choose $\tilde{\alpha}_C$ this range.
- Determine the $\tilde{\beta}_C$ parameter corresponding to r_0 and $\tilde{\alpha}_C$ using the method in [4].
- Set $\tilde{\lambda} = \tilde{\lambda}_+$, $\tilde{\alpha} = 3\tilde{\alpha}_C/4$, $\tilde{\beta} = \tilde{\beta}_C/4$, and $\tilde{D} = w/4$.
- Choose λ_C appropriately for the application and multiply $\tilde{D}$, $\tilde{\lambda}$, $\tilde{\alpha}$, and $\tilde{\beta}$ by the chosen value.

The bottom two rows of figure 1 show the results of gradient descent using E_{G} with parameters chosen by the above procedure, based on the HOAC parameters used in the first row, the better to illustrate the equivalence between the HOAC and phase field models. In the second row, the initial value of ϕ was equivalent to that used in the experiment shown in the first row. The evolution is very similar to the HOAC evolution. In the third row, the initialization was the neutral initialization plus Gaussian noise of very small amplitude. As can be seen, the phase field evolves towards a set of circles with the prescribed radius.

5. LIKELIHOOD ENERGY AND ENERGY MINIMIZATION

We use E_{G}, with parameters fixed as described above, as a prior model for the region R of the image domain corresponding to tree crowns. To complete the model, we also need a likelihood energy $E_{\mathrm{I}}(I,R)$. It is easy to reformulate active contour likelihoods as phase field models via the dictionary: normalized inward-pointing boundary normal vector $\partial\phi/2$; boundary characteristic function $|\partial\phi|^2$; region characteristic function $\phi_+ = (1+\phi)/2$; region complement characteristic function $\phi_- = (1-\phi)/2$.

We will model the image in R, and in the background $\bar{R}$, using Gaussian distributions. We add a term that predicts high gradients along the boundary ∂R:

$$E_{\mathrm{I}}(I,R) = \int_\Omega dx \left\{ \lambda_I\, \partial I \cdot \partial\phi + \frac{(I-\mu)^2}{2\sigma^2}\phi_+ + \frac{(I-\bar{\mu})^2}{2\bar{\sigma}^2}\phi_- \right\}.$$

Note that pixel values are independent except at the boundary between the tree crowns and the background. This independence results from the resolution of the images we will use, which is about 50cm/pixel. At this resolution there is no real texture information in the tree crown areas, while the background is varied as to make anything other than a broad maximum entropy distribution infeasible.

Having defined likelihood and prior energies, we then define the total energy for tree crown extraction as $E =$

$E_I(I,R) + E_G(R)$.[2] To minimize E we use standard gradient descent. The functional derivatives of all terms except E_{NL} are standard. The functional derivative of E_{NL} is

$$\frac{\delta E_{NL}}{\delta \phi}(x) = \beta \int_{\Omega} dx' \, \partial^2 G(x - x') \phi(x') \, . \tag{5}$$

Here we see explicitly the particular advantage of the phase field formulation for HOAC energies. Instead of the complex evaluation of the force due to E_Q described by Rochery et al. [11], involving, at each iteration, contour tracing, contour integration, and force extension, the equivalent force arising from E_{NL} can be computed with a simple convolution. It can, for example, be evaluated in the Fourier domain. Implementation is thereby made much easier, and execution much faster. Execution time for the HOAC formulation scales as the square of the boundary length, which in turn scales as the number of trees, which in turn scales as the number of pixels. Thus execution time for the HOAC formulation can be expected to scale as the number of pixels squared. In contrast, execution time for the phase field formulation scales as the number of pixels. For large images, then, the advantage of the phase field formulation in practical terms is obvious.

6. EXPERIMENTAL RESULTS

As stressed in section 1, tree crown extraction is an important forestry application, and it has been studied in several papers. Gougeon [3] uses a valley following method, based on a series of rules. Larsen [6] introduces a species-specific method based on the matching of 3D tree templates. Both these, and other similar methods, are local, in that they essentially look for local maxima of ceratin features. Perrin et al. [8] use a more global method, modelling tree crown configurations as a marked point process. One advantage with respect to the current method is that overlapping trees can be handled easily. One disadvantage is that trees are represented by ellipses: their outlines are not found.

The image data consists of the infrared channel of colour infrared aerial images. The images are of plantations in the 'Saône et Loire' region in France, and were provided by the French National Forest Inventory (IFN).

We will compare the 'gas of circles' phase field model with a CAC model ($E_{C,I} + E_{C,0}$), and with the HOAC 'gas of circles' model ($E_{C,I} + E_{C,G}$), where $E_{C,I}$ is the contour equivalent of E_I. The CAC and HOAC code is in C++, while the phase field code is in Matlab. This should be born in mind when comparing execution times.

It is useful also to compare the number of free parameters in these models. First, the parameters μ, σ, $\bar{\mu}$, and $\bar{\sigma}$ are learned from examples using maximum likelihood, and then fixed. For the CAC, this leaves three free parameters: λ_I, λ_C, and α_C. To count the number of free parameters for the HOAC and phase field models, we note that: w is fixed *a priori*; r_0 is fixed by the application; we can always choose $d = r_0$; $\tilde{\beta_C}$ is determined from $\tilde{\alpha_C}$ and r_0; the phase field parameters are determined once the contour parameters are chosen. This means that the only truly free parameters are λ_I, $\tilde{\alpha_C}$ and λ_C (or equivalently λ_I, D, and α). In addition, for the phase field model, $\tilde{\alpha_C}$ is constrained. Thus both the HOAC and phase field 'gas of circles' models have three effectively free parameters, the same number as the CAC model. The free parameters for each model, in common with most variational and many other methods, were fixed empirically (separately for each model) to give good results.[3]

Figure 2(a) shows an image (105×236) of a regularly planted poplar stand. Figure 2(b) shows the best segmentation result obtained using a CAC model. Without prior knowledge of the shape, the segmentation is poor: there are many misclassified and fused objects. Figure 2(c)shows the best result obtained using the HOAC model. Although the result is significantly better than the previous one, the execution time was 152 minutes. Figure 2(d) shows the best result obtained using the phase field 'gas of circles' model. The result, while still not perfect, is an improvement over the HOAC result, showing fewer misclassified tree crowns, and the execution time was less than 1 minute.

Figure 3(a) shows an image (128×128) of a second, less regularly planted poplar stand. The challenge of this image is that the tree crowns sometimes appear connected, and their crowns have varied intensities. The best result obtained using a CAC model is shown in figure 3(b). Several crowns are merged together, and the boundary is rather noisy. The best result obtained using the HOAC model is shown in figure 3(c). It took 96 minutes to compute. Figure 3(d) shows the best result obtained using the phase field model. Again it is an improvement on the HOAC result, with fewer fused tree crowns, while it took only 15 seconds to compute.

7. CONCLUSION

Based on the experimental results reported here, and others, it seems that the phase field 'gas of circles' model constitutes a significant improvement over its HOAC version, the latter in its turn producing much better results on the tree crown extraction problem than a CAC model. The phase field model outperforms the HOAC model both in the quality of results obtained, and in particular in terms of computation time: in our experiments, the phase field implementation was two orders of magnitude faster than the contour implementation.

The phase field 'gas of circles' model, combined with suitable likelihood energies, should be useful in a number of other applications, for example the extraction of craters and missile silos from remote sensing imagery, or of cells and organisms from medical and biological imagery, indeed anywhere that a number of circular objects need to be extracted.

References

[1] D. Cremers, T. Kohlberger, and C. Schnörr. Shape statistics in kernel space for variational image segmentation. *Pattern Recognition*, 36(9):1929–1943, September 2003.

[2] A. Foulonneau, P. Charbonnier, and F. Heitz. Geometric shape priors for region-based active contours. *Proc. IEEE International Conference on Image Processing (ICIP)*, 3:413–416, 2003.

[3] F. A. Gougeon. Automatic individual tree crown delineation using a valley-following algorithm and rule-based system. In D.A. Hill and D.G. Leckie, editors,

[2] We ignore the normalization constant $Z(R) = \int DI \, e^{-E_I(I,R)}$ since in our case it merely changes λ_C and α_C.

[3] Parameter values for the CAC, HOAC, and phase field models are shown in the figure captions when each result is mentioned, in the forms: $(\lambda_I, \lambda_C, \alpha_C)$, $(\lambda_I, \lambda_C, \alpha_C, \beta_C)$, and $(\lambda_I, \lambda, \alpha, \beta, D)$ respectively. The values of the other, common parameters are shown when the data is mentioned, in the form $(\mu, \sigma, \bar{\mu}, \bar{\sigma}, r_0)$.

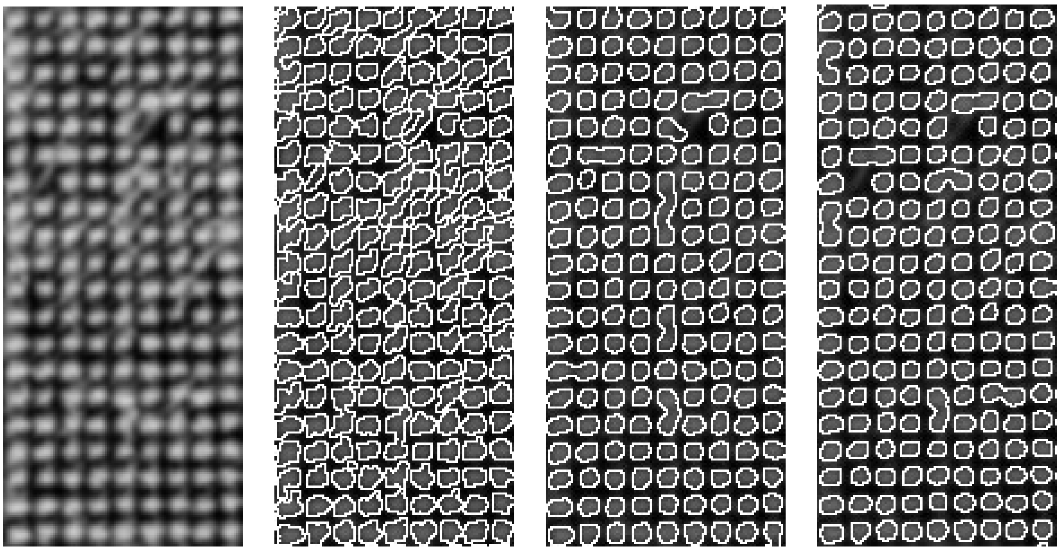

(a) (b) (c) (d)

Figure 2: Experimental results: (a) an image of poplars ©IFN $(0.86, 0.06, 0.43, 0.2, 3.5)$; (b) the best result with a CAC model $(35000, 100, 500)$; (c) the best result with the HOAC 'gas of circles' model $(1200, 20, 100, 82)$; (d) the best result with the phase field 'gas of circles' model $(1200, 239, 22.5, 16.8, 150)$.

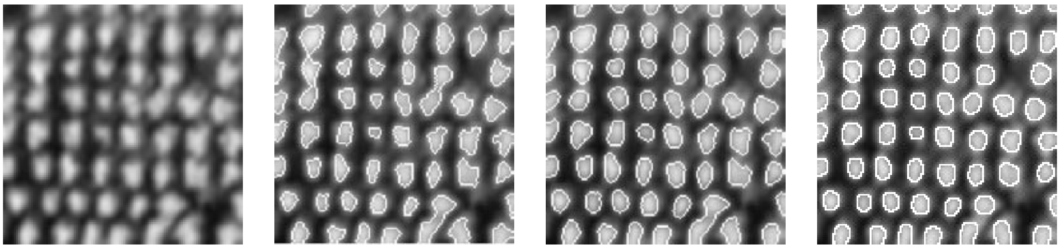

(a) (b) (c) (d)

Figure 3: Experimental results: (a) an image of poplars ©IFN $(0.71, 0.04, 0.27, 0.175, 4.2)$; (b) the best result with a CAC model $(880, 13, 73)$; (c) the best result with the HOAC 'gas of circles' model $(100, 6.7, 39, 31)$; (d) the best result with the phase field 'gas of circles' model $(100, 24.9, 5.63, 2.59, 18.8)$.

Proc. Int'l Forum on Automated Interpretation of High Spatial Resolution Digital Imagery for Forestry, pages 11–23, Victoria, British Columbia, Canada, February 1998.

[4] P. Horváth, I. H. Jermyn, Z. Kato, and J. Zerubia. A higher-order active contour model for tree detection. In *Proc. International Conference on Pattern Recognition (ICPR)*, Hong Kong, China, August 2006.

[5] M. Kass, A. Witkin, and D. Terzopoulos. Snakes: Active contour models. *International Journal of Computer Vision*, 1(4):321–331, 1988.

[6] M. Larsen. Finding an optimal match window for Spruce top detection based on an optical tree model. In D.A. Hill and D.G. Leckie, editors, *Proc. of the International Forum on Automated Interpretation of High Spatial Resolution Digital Imagery for Forestry*, pages 55–66, Victoria, British Columbia, Canada, February 1998.

[7] M.E. Leventon, W.E.L. Grimson, and O. Faugeras. Statistical shape influence in geodesic active contours. In *Proc. IEEE Computer Vision and Pattern Recognition (CVPR)*, volume 1, pages 316–322, Hilton Head Island, South Carolina, USA, 2000.

[8] G. Perrin, X. Descombes, and J. Zerubia. A marked point process model for tree crown extraction in plantations. In *Proc. IEEE International Conference on Image Processing (ICIP)*, Genova, Italy, September 2005.

[9] M. Rochery, I. H. Jermyn, and J. Zerubia. Higher order active contours and their application to the detection of line networks in satellite imagery. In *Proc. IEEE Workshop Variational, Geometric and Level Set Methods in Computer Vision*, at ICCV, Nice, France, October 2003.

[10] M. Rochery, I. Jermyn, and J. Zerubia. Phase field models and higher-order active contours. In *Proc. IEEE International Conference on Computer Vision (ICCV)*, Beijing, China, October 2005.

[11] M. Rochery, I. H. Jermyn, and J. Zerubia. Higher-order active contours. *International Journal of Computer Vision*, 69(1):27–42, 2006.